Demonstrating the Reverse Greenhouse Effect in the Laboratory – Part 1

Hermann Harde, Michael Schnell

Abstract

We present first quantitative studies demonstrating and using the principle of the reverse or so-called negative Greenhouse-Effect (GH-effect). The common GH-effect is running backwards, when air is warmer than a solid body with which it exchanges Infrared (IR) radiation. In this case, Greenhouse Gases (GH-gases) contribute to cooling of the air and to an increase in the outgoing IR radiation, which is detected by sensors on a cooled plate. With a series of laboratory experiments, it is shown that the IR radiation of GH-gases is not an "ominous" phenomenon but quite real and can be verified also under regular pressure conditions. The results were recently published in the journal *Science of Climate Change* [1] and are presented here in a slightly shortened, easy-to-understand form. Since the investigations are quite extensive, the studies are divided into two parts.

In this first part we consider some theoretical aspects of general interest: Why is the much stronger CO_2 band of 4.3 µm compared to the 15 µm band, insignificant for heat transport, why is water vapor the dominant greenhouse gas, and why is in a laboratory experiment – like an iceberg – only seen the tip of the gas radiation.

We explain how the negative GH-effect in Antarctica contributes to cooling of the planet. We also support the thesis that the temperature of the water planet Earth is mainly determined by evaporation, convection and cloud cover and not by infrared radiation.

In addition, the general concept of experimental investigations and initial tests with the new apparatus are presented. It turns out that the experimental set-up can also detect water vapor radiation, which was not possible in our previous studies [2]. This opens up new perspectives for investigating the superposition of water vapor radiation with that of other greenhouse gases.

In the second part, it is shown that CO_2, methane and nitrous oxide spontaneously convert heat of their environment to IR radiation, this also at normal air pressure and depending on the gas concentration, while water vapor exerts a damping effect.

Measurements and radiation transfer calculations are in good agreement when the interfering background radiation of the apparatus, and unavoidable transmission losses are taken into account.

Most convincing, the negative greenhouse effect is demonstrated using Freon 134a, an extremely effective greenhouse gas. A strong increase in IR emissions combined with a significant cooling of the ambient air—even with small amounts of freon—leaves no doubt: The thesis of thermalization or radiation-free deactivation is falsified according to K. Popper's definition.

1. Introduction

Greenhouse gases (GH-gases) are well known as absorbers of thermal radiation, proven by countless infrared spectra. According to Kirchhoff's radiation law, however, these gases can also be IR emitters. But this law is repeatedly questioned because, in contrast to condensed matter, the atmosphere – apart from aerosols and water droplets – essentially consists of freely moving molecules. Depending on the molar mass, temperature and pressure, the molecules travel at sound speed or slightly above. Because of this speed and their enormous number of around $2.7 \cdot 10^{25} = 27$ quadrillion molecules per cubic meter of air, these particles are continuously exposed to collisions of several GHz.

When a parcel of air is lifting up in the atmosphere, it is expanding and cooling down due to this volume work. As a result , less molecules at lower speed are found at higher altitudes in one cubic meter of air, so that the number of collisions decreases.

From this critics have concluded that GH-gases in the lower atmosphere are only absorbers and no or only weak emitters. They only acquire the property of a good emitter at higher altitudes, in the tropopause and stratosphere, where they contribute to the IR radiation to space. As an explanation, they state that in the lower troposphere, collision processes in the form of hyperelastic collisions suppress spontaneous emissions. According to this, the absorbed energy would be converted mainly to kinetic energy as heat, which is called thermalization or radiation-less deactivation.

This interpretation ignores that there are also inelastic collisions which have the opposite effect to hyperelastic collisions. These collisions extract kinetic energy from the gas mixture and use this energy to excite GH-gas molecules to rotational-vibrational states. These processes ultimately lead to thermal radiation largely independent and parallel to the superelastic collisions. This is referred to as thermal background radiation (Harde 2013 [4], Chapter 2.5). The emission is determined by the air temperature and thus the population of excited levels according to a Boltzmann distribution. This is the main reason why the radiation intensity decreases significantly with increasing altitude. For example, at an altitude of 11 km, it is only 12 % of the CO_2 intensity observed in a 100 m thick gas layer near the ground.

For several years now, these two opposing views have been clashing in EIKE articles, despite the existence of detailed laboratory experiments confirming the greenhouse effect (see Harde, Schnell 2024 and [2]). But perhaps some doubters can still be convinced by our laboratory experiments that the three most important infrared-active gases in the atmosphere – CO2, methane and nitrous oxide – spontaneously generate IR radiation at the expense of the heat of their environment even at normal pressure.

2. Theoretical Basics

GH-gases can absorb and re-emit radiation in the medium and long-wave IR spectral range. This spectral range extends on a wavelength scale λ from approximately 4 µm to the cm range. Within this spectral interval, the most important GH-gases in the atmosphere such as water vapor (WV), carbon dioxide (CO_2), methane (CH_4), nitrous oxide (N_2O) and ozone (O_3) have a total of 722,000 spectral lines. Many of these lines are very faint, but due to the long propagation paths in the atmosphere, they also contribute significantly to the interaction with radiation (Fig. 1).

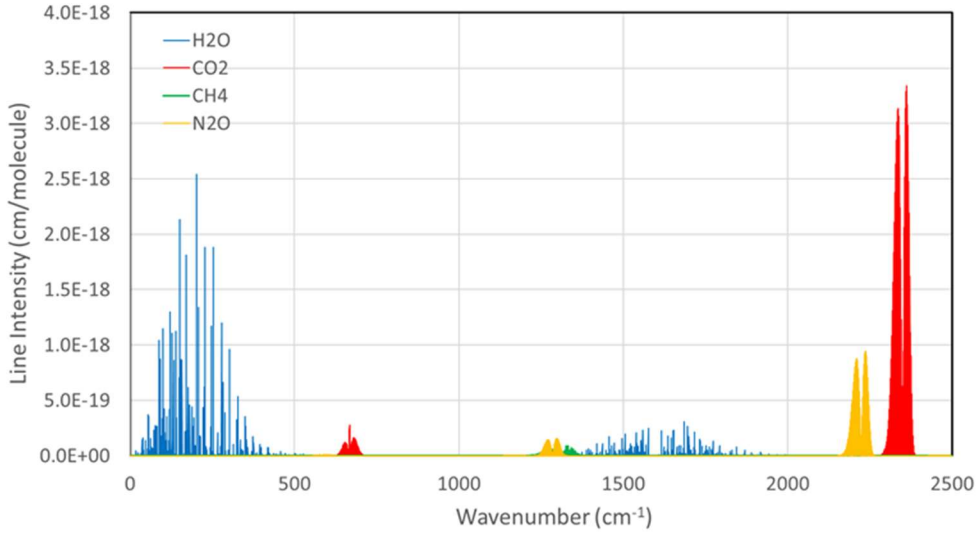

Fig.1: Line intensities of the greenhouse gases WV, CO_2, CH_4 and N_2O over the spectral range from 0 – 2500 cm^{-1}. This corresponds to a wavelength range of ∞ - 4 µm. The values apply to a temperature of T = 44 °C.

In spectroscopy, it is common to specify absorption lines by wavenumbers $\tilde{\nu} = 1/\lambda$, the reciprocal value of the wavelength. They indicate how many oscillations fit to one centimeter and are expressed in units cm^{-1}. As for light waves it holds $c = \lambda \cdot \nu$ (c - speed of light, ν - frequency of light), wavenumbers as $\tilde{\nu} = 1/\lambda = \nu/c$ or $\nu = c \cdot \tilde{\nu}$ represent a frequency scale, where 1 cm^{-1} is equivalent to 30 GHz. This has some consequences that can be confusing: the strong asymmetric CO_2 stretching vibration at 4.3 µm is now on the right side at 2 326 cm^{-1} and the weaker CO_2 bending vibration at 15 µm on the left side at 667 cm^{-1} (Fig. 1, red lines).

However, the line intensity in Fig. 1 does not say too much about its share in the IR emission of an air parcel, which is additionally determined by the thermal population of excited states according to a Boltzmann distribution and Planck's law (see Fig. 2; Harde 2013, chap. 2.3 [4]).

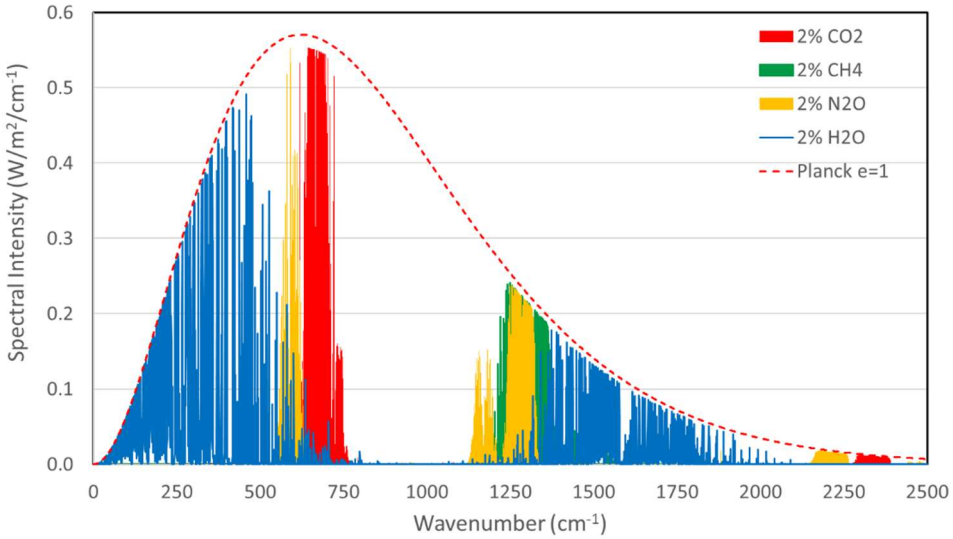

Fig.2: Emission spectra of WV, CO_2, CH_4 and N_2O over a propagation length of 70 cm for concentrations of 2 %, each in air for a gas temperature T = 44 °C and a pressure of 1013 hPa.

The red, dashed line displays the Planck distribution of a blackbody emitter at a temperature of 44 °C (emissivity ε = 100 %), corresponding to the temperature of the gases during the investigations. For each spectral line this is the maximum possible radiation density (spectral intensity) under these conditions, more is not possible. This is the reason why the very strong CO_2 lines (Red) in Fig. 1 around 2300 cm^{-1} with only 1.3 W/m² play an absolutely subordinate role compared to a theoretical total emission of CO_2 with 28.8 W/m². In contrast, the relatively small CO_2 emissions around 670 cm^{-1} with their many rotation lines practically coincide with the maximum and the band center already shows complete saturation over a propagation length of 70 cm. It significantly determines the share of CO_2 to the GH-effect (Red lines).

Nitrous oxide (N_2O, orange) with an own emission of 29.2 W/m², is additionally masked by methane (CH_4, Green) with 11.1 W/m², and the strongest band of N_2O around 2250 cm^{-1} has hardly any influence on the total emission.

It is also clear that not CO_2 but water vapor (WV, Blue) with a total emission of 42.2 W/m² is the dominant greenhouse gas and superimposes larger parts of the other gases, although same concentrations were used for this comparison. While the individual contributions of the four gases add up to an intensity of 111.3 W/m², the total effective intensity is only 75.8 W/m² and is therefore 32 % lower.

This loss occurs when the different gases are overlapping in their emission bands and are radiating on the same wavenumbers, as especially observed for water vapor, which has also been proven experimentally (see Part 2).

In the lower atmosphere, the concentration of water vapor on average is 35 times higher than that of CO_2. This results in such a strong overlap that the regularly expected radiation of CO_2 with 83 W/m² (at

a ground temperature of 15 °C) only contributes additional 22 W/m², i.e. about a quarter. On the other hand, WV alone already generates 281 W/m², and together they radiate 304 W/m² towards the surface. When we also consider that the increasing CO_2 concentration from 280 to 420 ppm over the Industrial Era only contributes additional 2.2 W/m² (increase from 301.4 to 303.6 W/m²) due to saturation effects on the molecular transitions, and that this fraction is further reduced to about 1.3 W/m² (328.1 to 329.4 W/m²) under clouds (cloud cover of 66% and cloud height of 5 km), the contribution of CO_2 to the total back-radiation is indeed almost negligible.

3. Experimental Concept and Analysis of Heat Flux

It is undeniable that greenhouse gases are also emitters, because the energy input of the Sun can ultimately only leave the Earth-Atmosphere-System (EASy) in form of electromagnetic radiation. The only point of contention is whether this also works at normal pressure. This is exactly where the idea for the new laboratory experiment comes in. An experiment under standard pressure conditions does not require any special measures. Therefore, without too much effort it is possible to investigate what can be observed when some smaller amount of an IR-active gas is added to a slightly warmed air volume.

To verify this, all you need is a heated air cylinder and a cooled plate PC with a radiation detector. Both parts are placed vertically on top of each other to prevent convection (Fig. 3). A polyethylene (PE) foil between the cylinder and the cooled plate reduces direct heat conduction, so that the heat is mainly transferred by infrared radiation to the cooled plate. This heat flux Q is registered by two sensors, TD and VP, which are located on the PC disk (for a detailed description of the apparatus, see Part 2).

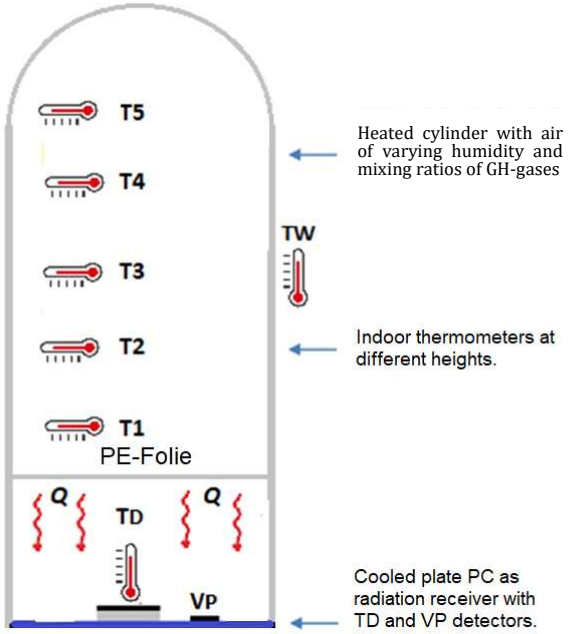

Fig.3: Schematic experimental setup

The experimental setup allows for a continuous heat flow in only one direction, from the warm air cylinder to the colder PC disk. A possible violation of the second law of thermodynamics is thus ruled out per se, which eliminates the main argument of the skeptics.

Different to [2], the cylinder is not heated electrically, but indirectly by a jacket heater with thermostatized water T_W of 51°C. Between the TW jacket heater and the cylinder wall is a 2 mm thick polystyrene insulation, which causes a reduced heat flow from the heating water to the inner air of the cylinder. Due to this insulating layer, the cylinder temperatures T_1 to T_5 not only depend on the heating TW, but also on the outgoing heat flux Q. This can be demonstrated experimentally by a gradual increase of the T_W

temperature. Without heat flux Q to the PC disk, the heating temperature T_W and the temperatures T_1 to T_5 *would have to* adapt after some delay. But it turns out that with increasing T_W temperature, the differences become larger, which is caused by an increasing heat flux Q (Fig. 4a). Most of the heat is emitted at the T1 position. This interpretation is confirmed by an increasing heat flux Q, which is registered by the detectors TD and VP (Fig. 4b).

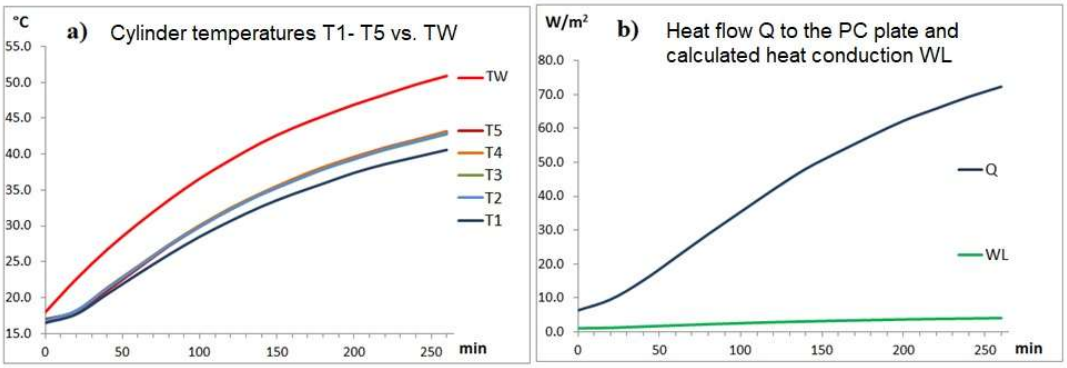

Fig. 4: a) Increase of temperatures T_1 – T_5 with increasing jacket temperature T_W, b) Verification of the heat flux Q with increasing temperature by two sensors TD and VP and calculation of the mechanical heat conduction W_L to the PC plate, H_2O = 0.15 vol.-%.

The heat flux Q to the PC plate consists of the radiation I_0 and the outer heat conduction W_L from the cylinder base to the PC plate. The gradual increase in T_W was done in small increments with a rest period of 20 minutes. At the end of this rest phase, there is again an approximate thermal equilibrium. Due to the stationary air layers, mechanical heat conduction can be calculated according to

$$W_L = A \cdot \Delta T \cdot \lambda_{air}/L\,. \qquad (1)$$

Here λ_{air} = 0.026 W/m/K is the thermal conductivity for air, $\Delta T = T_1 - T_C$, A = 0.086 m² the cylinder cross-sectional area and L = 20 cm the distance T1 – PC. According to this, the heat flux W_L accounts for only about 6% of the total heat flux Q (Fig. 4b, green curve).

So, about 94% of the heat flux Q is transferred by IR radiation I_0. On the one hand, this is the desired energy transport, but on the other hand, it is also bad news, because this I_0 radiation is the background radiation of the air-filled cylinder without GH-gases. The background radiation superimposes and obscures the radiation of the GH-gases, so that only the tip of the gas radiation is visible during these experiments, similar to an iceberg (Chapter 4). This is the main reason why the detection of gas radiation is so difficult and why previous experiments have failed because of this problem.

At first glance, a horizontally placed polystyrene box seems to be a convenient solution, as it is commercially available and easy to process. For example, Seim and Olsen [5] have tried to test our previous studies on the greenhouse effect [2] with such a setup. They were able to confirm that CO_2 causes some temperature rise, but the levels were much smaller than we found. The various reasons for this failure are explained in Schnell & Harde (2025) [3].

4. Water Vapor Radiation

For the experiment in the previous chapter (Fig. 4), dried air with a concentration of about 0.15 % was used inside the cylinder. Repeating this experiment with normal laboratory air at a WV concentration of 1.1 % gave an increase of the outgoing heat flux Q of 5 – 8 W/m² (Fig. 5).

This increase in Q is caused by the IR radiation of water vapor. This opens up new possibilities for investigating the role of water vapor in the greenhouse effect (see Part 2): either the cylinder air is left untreated, dried or additionally moistened for a measurement. In this way, three WV concentrations of

0.15, 1.1 and 1.9 vol. % could be achieved in the cylinder. However, additional humidification with 1.9 % water vapor is difficult, as water vapor condenses easily at uncontrollable thermal bridges. Therefore, the higher concentration was only realized for the CO_2 investigation.

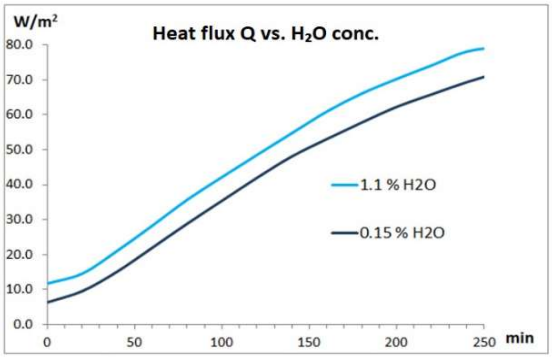

Fig. 5: Heat flux Q at 1.1 and 0.15% water vapor.

Part 2 shows that concentrations of up to 8% by volume are required to detect the emission of CO_2, methane and nitrous oxide. As explained above, this cannot be achieved with steam. Therefore, water vapor is not investigated as a greenhouse gas, but its influence on the other GH-gases with relatively low WV concentrations (Part 2).

5. Background Radiation and Transmission Losses

The great challenge measuring the gas radiation is to detect it on the large background radiation from the cylinder walls. The inner surface of the cylinder is more than 10 times larger than the radiation area, and together with multiple reflections makes the cylinder a cavity radiator, which emits significantly higher intensity than a flat plate of the same material, this despite a very low emissivity of the polished aluminum walls of only about 5% (see cavity radiators, e.g. Atkins & Friedman 2011[6]).
To get an idea of the gas to background radiation, Fig. 6 displays a calculation for CO_2 and WV, superimposed by the wall radiation. The total emission of the cylinder walls can be characterized by an effective emissivity ε_{eff} = 42 %, and the losses to the detectors – caused by a limited acceptance angle and the transmission of the PE foil – by a dissipation factor of $V_\Omega \approx 40$ %. The stronger drops at 740 cm^{-1}, 1,350 cm^{-1} and 1,400 cm^{-1} are caused by the transmission losses of the PE foil at these wavenumbers.

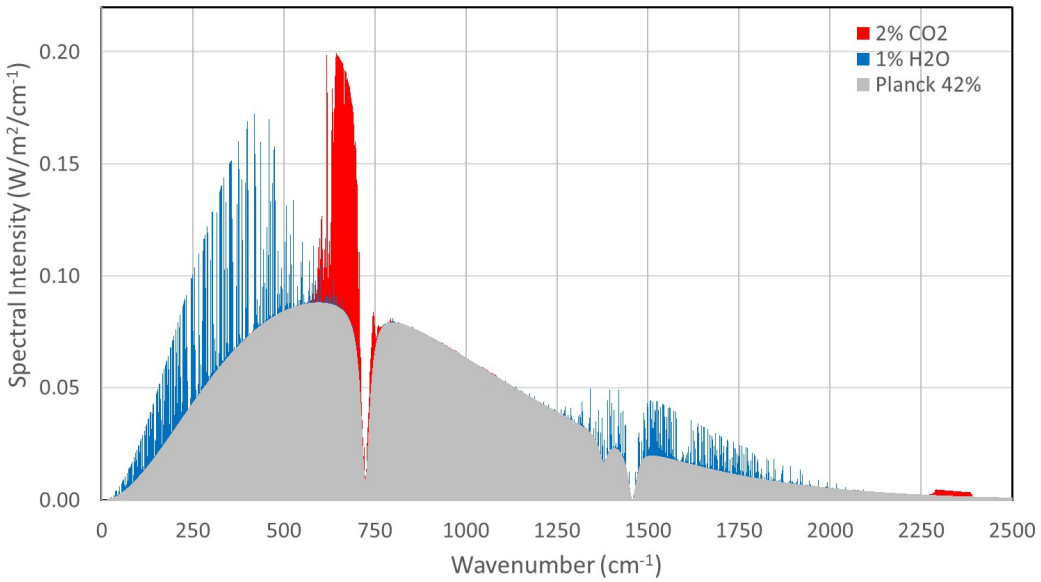

Fig. 6: Spectral intensity as a function of the wavenumber for 2 % CO_2, 1 % H_2O, L = 70 cm, ε = 42% and V_Ω = 40 % with a total intensity of 95.6 W/m².

The emission from the walls (Grey) and water vapor (Blue) together give 90.3 W/m^2. With additional 2 % of CO_2, this intensity increases to 95.6 W/m^2. This increase of 5.3 W/m^2 is not more than 18.4 % of the expected CO_2 radiation of 28.8 W/m^2, which would be observed without an overlap with the other radiation sources. Despite the optimized experimental setup, the vertical setup and the polished aluminum surface, only the tip of the CO_2 gas radiation is visible (red lines), like an iceberg.

6. The Negative Greenhouse Effect

6.1 Definition of the GH-Effect and Simplified Derivative

According to Thomas & Stamnes (1999) [7] and the actual assessment report of the IPCC, AR6 [8], the atmospheric greenhouse effect is defined as the difference of the radiation intensities emanating from the Earth's surface F_S and the upper atmosphere F_{TOA} (Top of the Atmosphere).

The mean surface radiation can be approximated by the Stefan-Boltzmann law:

$$F_S = \varepsilon_S \cdot \sigma \cdot T_S^4, \tag{2}$$

with ε_S as emissivity and T_S as temperature of the Earth's surface and $\sigma = 5.67 \cdot 10^8$ W/m^2/K^4 as Boltzmann constant.

The radiation to space F_{TOA} consists partly of the Earth's radiation not absorbed by the atmosphere (term 1), plus the radiation emitted by the atmosphere itself (term 2):

$$F_{TOA} = \varepsilon_S \cdot (1 - \alpha_A) \cdot \sigma \cdot T_S^4 + \varepsilon_A \cdot \sigma \cdot T_A^4 \ , \tag{3}$$

with α_A as absorptivity and T_A as temperature of the atmosphere.

Assuming a simple two-layer model (see also Schmithüsen et al. [9]) and replacing the absorptivity α_A by the numerically identical emissivity ε_A , the greenhouse effect (*GHE*) can be expressed as (see [1] for further details):

$$GHE = F_S - F_{TOA} = \varepsilon_A \, \sigma \left(\varepsilon_S \, T_S^4 - T_A^4 \right). \tag{4}$$

The emissivity ε_S includes all IR-active gases and depends on their concentrations.

6.2 Different Impacts of the GH-Effect

The temperature difference between the Earth's surface and the atmosphere determines whether the GH-effect warms or cools, whether it is positive or negative (Eq. 4). We distinguish three scenarios:

A) ($T_S > T_A$): Usually, the Earth's surface is warmer than the troposphere, and the temperature over the troposphere is declining with increasing altitude, in average 6.5 °C/km. The greenhouse effect is positive and has a warming effect. Under these conditions the atmosphere hinders the IR radiation transport to space, and the intensity F_{TOA} is less than the original Earth's radiation F_S. Thus, the greenhouse effect is a kind of thermal insulation of the radiative transport (here).

B) ($T_S = T_A$): At the same temperatures and $\varepsilon_S = 1$ there would be no greenhouse effect, as Richard Lindzen has aptly formulated:
„*It is an interesting curiosity that in the case convection had produced a constant temperature, there would be no greenhouse effect*“ (here).

C) ($T_S < T_A$): When the Earth is colder than the atmosphere, there is a negative GH-effect. In this case, the radiation to space F_{TOA} is greater than that of the Earth's radiation F_S. The energy required for this additional radiation is taken from the atmosphere, which leads to cooling. Such a constellation is realized in the current experiments, on the one hand to show the emission properties of greenhouse

gases and on the other hand to prove the existence of a negative GH-effect on a model scale.

The negative greenhouse effect also occurs under inversion weather conditions or during nightly cooling, when the near-Earth's air is warmer than the ground.

The negative effect at the Earth's poles is climatically significant, as often the interior of the Antarctica's surface is colder than the air layers above. This increases the long-wave radiation in these regions and intensifies the cooling of the planet (Schmithüsen, 2015 [9], see also Winter Gatekeeper Hypothesis.

A special case is heat, released by uplifting air as sensible or latent heat at higher altitudes (around 5 km or more). Here, particularly CO_2 causes cooling and thus a negative greenhouse effect, as the cold universe with around -270 °C is the direct radiation partner and only a small amount of water vapor exists at higher altitudes (see also: Harde [4], Section 3, Cooling in the stratosphere, Fig. 10).

To avoid a misunderstanding: The recognition of the GH-effect is not a plea for a climate catastrophe, but merely the existence of a real atmospheric phenomenon. For the heat flows in the atmosphere, however, the greenhouse effect is of secondary importance. The Earth, 70% covered by water, controls its surface temperature mainly through evaporation, convection and, above all, by clouds. Vahrenholt argues that a substantial fraction of recent warming may be attributable to reduced cloud cover driven by aerosol changes rather than greenhouse gases alone – a hypothesis that deserves serious consideration alongside the radiative forcing literature.

The formation of clouds depends critically on the existence of condensation nuclei, including the harmful sulfuric acid aerosols that form sulfur dioxide. Their reduction through flue gas desulfurization – a process that has measurably improved air quality across Europe and North America since the 1970s – has also reduced the aerosol load that previously suppressed incoming solar radiation. Several researchers, including Wild (2009) [10], Rosenfeld et al. (2014) [11] and Schilliger et al. (2024) [12] have documented a corresponding increase in surface solar radiation ("global brightening") that may have contributed to warming trends independent of greenhouse gas forcing. The climate consequences of aerosol reduction deserve more attention than they typically receive in mainstream attribution studies.

But there is also a significant natural influence on the cloud cover, as this can be derived from the Total Solar Irradiance (TSI) data and the solar wind with its impact on cosmic rays, which also affect the formation of clouds (see: Svensmark et al., 2016 [13]; Harde, 2022 [14]).

The importance of clouds or their lack can be easily demonstrated by looking at the areas with the highest recorded Earth temperatures so far. In these areas, there are neither clouds nor large amounts of water vapor. The latter is of particular importance for the CO_2 GH-effect, because according to the IPCC it is the so-called "water vapor feedback" that makes the harmless gas a global threat. The only strange thing is that the warmest places in the world are not the humid rainforests at the equator, but the dry or tropic deserts in the subtropics. The place with the highest ground temperature of 70 – 78 °C is the Dasht-e Kawir Desert in Iran with an annual rainfall of < 50 mm (here).

The Death Valley is one of the driest regions on earth. There, on July 10, 1913, the air had a temperature of 56.7 °C, the highest value ever measured there (here).

Of course, these temperatures are driven by the proximity to the equator, the clear sky with the maximum possible hours of sunshine and a dry soil without water evaporation. But also the downdrafts, which counteract cooling by convection.

In the presence of larger amounts of water vapor, temperatures look quite different. For example, despite their proximity to the equator and their high humidity, the daily maximum values in the tropical rainforests are only about 30 °C (here). Since moist air increases convection due to its low density, this particularly strong buoyancy leads to climate stability in the tropics and to a so-called tropical attenuation. As a result of the upwelling in the tropics, dry downdrafts are created in the subtropics. These

create additional areas of clear skies, so that the long-wave radiation can be emitted to space more efficiently (here). However, it must be admitted that in the tropics, in addition to evaporative cooling, cloud formation and the resulting reduced solar radiation as well as the almost daily rainfalls are responsible for the moderate day-night temperatures between 25 and 30 °C.

The oceans cannot keep up with the temperatures of the dry deserts. The warmest of them, the Indian Ocean, reaches a maximum of 28 °C (as of 2021) (here). This is not only due to its enormous heat capacity and thermohaline circulation (ocean currents that connect warm and cold oceans, also known as the global conveyor belt). Above all, however, it is due to its evaporative cooling, which leads to cloud formation and precipitation (see, e.g., Clauser, 2024 [15]), but also to a negative feedback for the CO_2 Equilibrium Climate Sensitivity ECS (Harde, 2017 [16], Subsec. 4.3.5). If humans intervene here, e.g. with well-intentioned measures for air purity, they cause more damage to the climate than through the release of CO_2 (here, here).

It bears noting that claims of an impending "boiling" of the oceans are not physically plausible. The boiling point of water at sea level is 100 °C (212 °F), and dissolved salts raise this further. A 1–2 °C increase in ocean surface temperature, while consequential for marine ecosystems, is an entirely different physical regime from boiling. The laws of thermodynamics are not subject to rhetorical revision.

References

1. H. Harde, M. Schnell 2025: The Negative Greenhouse Effect Part II: Studies of Infrared Gas Emission with an Advanced Experimental Set-Up, Science of Climate Change, Vol. 5.3., pp. 10-34. https://doi.org/10.53234/scc202510/03.
2. H. Harde, M. Schnell, 2022: *Verification of the Greenhouse Effect in the Laboratory*, Science of Climate Change, Vol. 2.1, 1-33. https://doi.org/10.53234/scc202203/10
3. M. Schnell, H. Harde, 2025: The Negative Greenhouse Effect Part I: Experimental Studies with a Common Laboratory Set-Up, Science of Climate Change, Vol. 5.3., pp. 1-9. https://doi.org/10.53234/scc202510/02
4. H. Harde, 2013: *Radiation and Heat Transfer in the Atmosphere: A Comprehensive Approach on a Molecular Basis*, International Journal of Atmospheric Sciences (Open Access), vol. 2013, http://dx.doi.org/10.1155/2013/503727
5. T.O. Seim, B.T. Olsen 2023: *The Influence of Heat Source IR Radiation on Black-Body Heating/Cooling with Increased CO_2 Concentration*, Atmospheric and Climate Sciences, 13, 240-254. https://www.scirp.org/journal/acs.
6. P. Atkins, R. Friedman, 2011: *Molecular Quantum Mechanics*, 5. Edition, Oxford University Press, Oxford, Schwarzkörperstrahlung | tec-science
7. G. E. Thomas, K. Stamnes, 1999: *Radiative Transfer in the Atmosphere and Ocean*, Cambridge Univ. Press, Cambridge, U. K., equation 12.19.
8. IPCC Sixth Assessment Report (AR6), 2021: V. Masson-Delmotte, P. Zhai, A. Pirani et al.: *Climate Change 2021: The Physical Science Basis. Contribution of Working Group I to the Sixth Assessment Report of the Intergovernmental Panel on Climate Change*, Cambridge University Press.
9. H. Schmithüsen, J. Notholt, G. König-Langlo, P. Lemke, T. Jung, 2015: *How increasing CO2 leads to an increased negative greenhouse effect in Antarctica*, Geophys. Res. Lett., 42, pp. 10422 –10428, https://doi.org/10.1002/2015GL066749
10. M. Wild, 2009: *Global dimming and brightening: A review*, J. Geophys. Res., 114, D00D16, https://doi.org/10.1029/2008JD011470.
11. D. Rosenfeld et al., 2014: *Global observations of aerosol-cloud-precipitation-climate interactions*, Rev. Geophys., 52, 750–808, https://doi.org/10.1002/2013RG000441.

12. L. Schilliger, A. Tetzlaff, Q. Bourgeois, L. F. Correa, M. Wild, 2024: *An investigation on causes of the detected surface solar radiation brightening in Europe using satellite data*, J. Geophys. Res.: Atmospheres, 129, e2024JD041101, https://doi.org/10.1029/2024JD041101.

13. J, Svensmark, M. A. B. Enghoff, N. J. Shaviv, H. Svensmark, 2016: *The response of clouds and aerosols to cosmic ray decreases,* Journal of Geophysical Research: Space Physics, Vol. 121.9, pp. 8152–8181, https://doi.org/10.1002/2016JA022689.

14. H. Harde, 2022: *How Much CO_2 and the Sun Contribute to Global Warming: Comparison of Simulated Temperature Trends with Last Century Observations*, Science of Climate Change, Vol. 2.2, pp. 105-133, https://doi.org/10.53234/scc202206/10.

15. J. Clauser, 2024: *The Cloud Thermostat Controls the Climate*, EIKE-Conference, Wien, https://eike-klima-energie.eu/2024/08/01/john-clauser-der-wolken-thermostat-reguliert-das-klima-deutsche-version/

16. H. Harde, 2017: *Radiation Transfer Calculations and Assessment of Global Warming by CO_2*, International Journal of Atmospheric Sciences, Volume 2017, Article ID 9251034, pp. 1-30, https://www.hindawi.com/journals/ijas/2017/9251034/, https://doi.org/10.1155/2017/9251034.